Available online at www.sciencedirect.com

SciVerse ScienceDirect

Energy Procedia 10 (2011) 313 – 322

Energy Procedia

European Materials Research Society Conference
Symp. Advanced Inorganic Materials and Concepts for Photovoltaics

Study of the Optical Properties of Sn-doped Sb_2S_3 Thin Films

F. Aousgi* and M. Kanzari

Laboratoire de Photovoltaïque et Matériaux Semi-conducteurs-Université Tunis-El Manar-ENIT BP 37, Le belvédère 1002-Tunis, Tunisie
Corresponding author: e-mail: aousgifethi@yahoo.fr

Abstract

Sn doped Sb_2S_3 thin films have been deposited by single source vacuum thermal evaporation onto glass substrates at substrate temperature Ts= 240 °C. The optical constants were obtained from the analysis of the experimental recorded transmission and reflectance spectral data over the wavelength range 300–1800 nm. It has been found that the refractive index dispersion data obeyed the single oscillator of the Wemple-DiDomenico model. By using this model, the dispersion parameters and the high-frequency dielectric constant were determined. The electric free carrier susceptibility and the carrier concentration on the effective mass ratio were estimated according to the model of Spitzer and Fan.

Keywords: X-ray diffraction ; Amorphous semiconductors; glasses; Vacuum deposition;Vacuum deposition.

1. Introduction

Sb_2S_3 is a member of V_2-VI_3 layered semiconductor family. In recent years a large number of studies have devoted to the physical properties of chalcogenides thin films due to their wide applications in optoelectronic devices [1, 2]. Among the available chalcogenides, pure and doped Sb_2S_3 thin films are used in solar energy conversion, thermoelectric cooling technologies and as photoconductive target type of television camera [3, 4]. This is mainly due to its direct band gap of about 1.78 - 2.5eV [5-6] and a high absorption coefficient (10^5 cm^{-1}). Due to these potential applications it is very important to

* Corresponding author. Tel.: +219 99 200 482; fax: +216 71 872 729.
E-mail address: aousgifethiahoo.fr.

doi:10.1016/j.egypro.2011.10.197

determine the structural, electrical and optical properties of this material. But in spite of these proprieties, Sb_2S_3 is usually presents high resistive. So to convert Sb_2S_3 in p or n type conductivity we shall dope it. In our previously works [7] we showed that $Sn_2Sb_2S_4$ thin films exhibit stable p-type conductivity. Consequently, Sn as a doping element can affects the conductivity type of the Sb_2S_3 thin films. Therefore for these reasons we chose to dope Sb_2S_3 with Tin (Sn) element.

In this paper, we studied the effect of Sn incorporation in Sb_2S_3 thin films grown by vacuum evaporation method at substrate temperature Ts= 240 °C. We report our investigations on the optical properties of amorphous thin films of Sb_2S_3 which were studied in the photon energy range 0-4 eV. The results of measurements of the optical properties of Sn-doped Sb_2S_3 thin films (% molecular weight 0% – 3%) give information regarding the absorption coefficient α, the band gap Eg, the extinction coefficient k, the refractive index n, the dispersion energy E_d, the energy of the effective dispersion E_0, the static refractive index n(0), the high frequency dielectric constant ε∞, the carrier concentration to the effective mass ratio N/m* and the electric free carrier susceptibility χ_e were estimated according to the model of Spitzer and Fan and Wemple–Di Domenico.

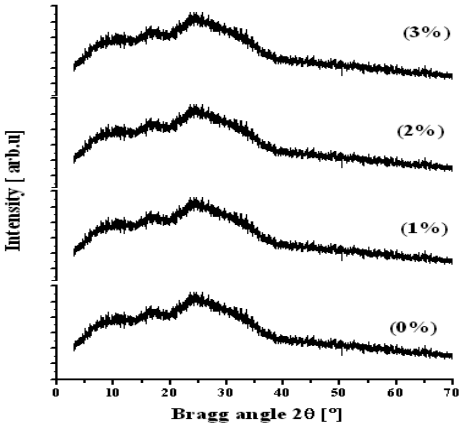

Fig. 1 XRD pattern of Sn-doped Sb_2S_3 thin films (% molecular weight 0% – 3%).

2. Experimental procedure

2.1. Synthesis of Sb_2S_3 ingots

Stoichiometric amounts of the elements of 99.999% purity Sb and S were used to prepare the initial ingot of Sb_2S_3. The mixture was sealed in vacuum in a quartz tube. In order to avoid explosions due to sulfur vapor pressure, the quartz tube was heated slowly (20 °C/h). A complete homogenization could be obtained by keeping the melt at 650°C for 48h; thermal expansion of the melt on solidification was avoided. X-rays of powder analysis showed that only homogeneous Sb_2S_3 phase was present in the ingot. Crushed powder of this ingot was used as raw material for the thermal evaporation.

2.2. Preparation of Sb_2S_3 thin films and doping process

Sb_2S_3/Sn thin films were prepared by co-evaporation of the Sb_2S_3 powder and the Sn element in a high vacuum system with a base pressure of 10^{-6} Torr. Sn of 4N purity was evaporated from thermal evaporator. An open ceramic crucible was used. Sn was deposite simultaneously during the deposition of

the Sb_2S_3 powder. Thermal evaporation sources were used which can be controlled either by the crucible temperature or by the source powder. The glass substrates were heated at 240 °C during the evaporation process. The amount of the Sn source was determined to be 0%–3% molecular weight compared with the Sb_2S_3 alloy source.

2.3. Characterization of the as-deposited Sb_2S_3 thin films

The optical characteristics were determined at normal incidence in the wavelength range 300 - 1800 nm using a Shimadzu UV/VIS/NIR-spectrophotometer. The film's thicknesses were calculated from the positions of the interference maxima and minima of reflectance spectra using a standard method [8]. The film thicknesses were found to be in the range 500-600 nm. The type of conductivity of the as-deposited Sb_2S_3 thin films was determined by the hot probe method and all the as-deposited films present high resistive values. The surface morphology and roughness of the films were examined means of atomic force microscopy (AFM) type Vecco model D3100. The hot probe method measurements were carried out in order to determine the conduction type of the samples.

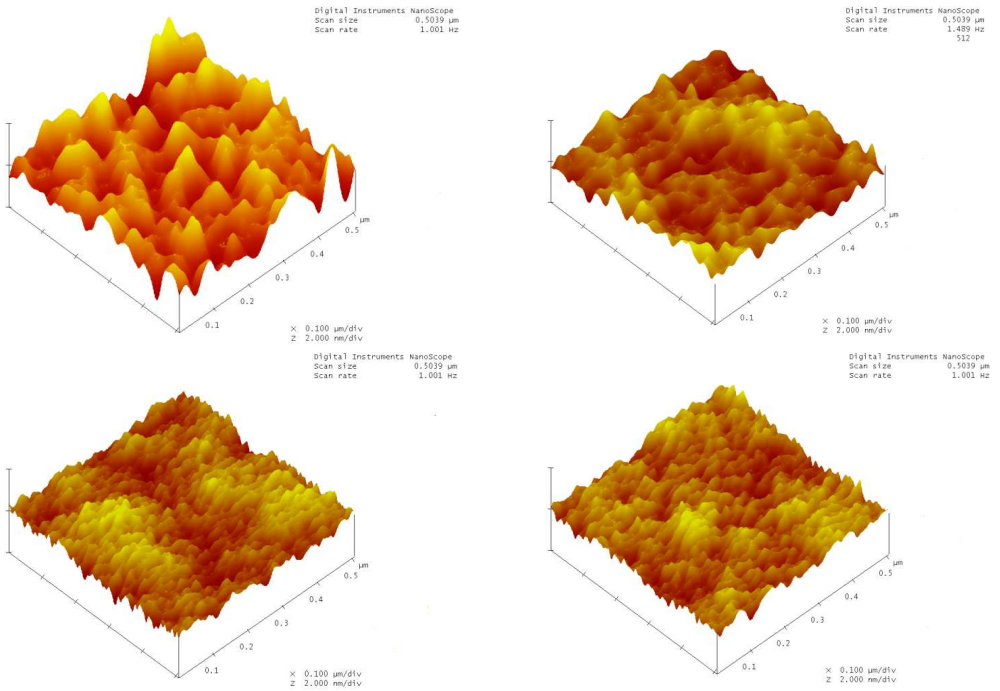

Fig. 2 AFM images of Sn-doped Sb_2S_3 thin films (% molecular weight 0% – 3%.

3. Results and discussion

3.1. Structural and morphological studies

The X-ray diffractograms of the undoped and Sn-doped Sb_2S_3 films are shown in Figures. 1. It is clear from Fig. 1 that the all investigated films formed at substrate temperature Ts= 240 °C have an amorphous nature, which agrees with the previous observations reported for all the substrate temperature ≤ 250 °C,

eg by N. Tigau et al [9-10] and our previous published work [5]. The amorphous nature of the film formed at low substrate temperature is due to the non-availability of sufficient thermal energy for the diffusion of adatoms on the substrate surface for the nucleation.

We studied surface morphologies of the Sb_2S_3 films by Atomic Force Microscopy (AFM). Fig. 2 shows their surface morphologies analyzed by AFM. The measured grain size and RMS roughness are given in Table 1. It is clear from the Table that the average grain size increases by increasing the Sn % molecular weight. The root mean square (RMS) values of surface roughness were found between 5.5 and 2.5 nm (Fig. 2). The roughness of the films shows distinct decrease by increasing the Sn % molecular weight.

Table 1. The grain size and roughness of undoped and Sn-doped Sb_2S_3 thin films.

Sb_2S_3/Sn	Grain size (nm)	Roughness (nm)
0 (%)	42	5.5
1 (%)	45	3.7
2 (%)	44	3.2
3 (%)	47	2.5

3.2. Optical properties of Sb_2S_3/Sn thin films

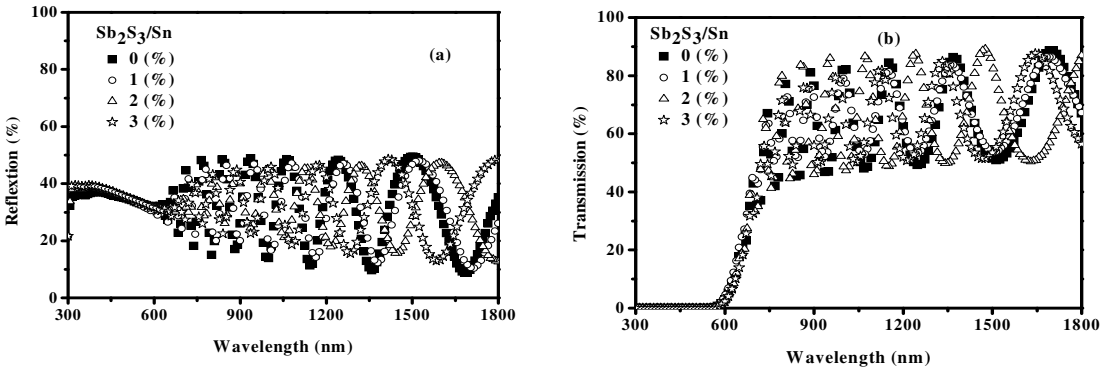

Fig. 3. Reflection (a) and transmission spectra (b) of undoped and Sn-doped Sb_2S_3 thin films.

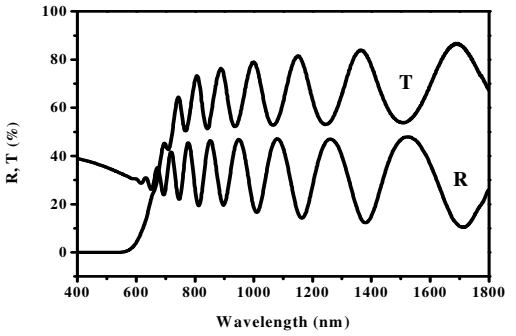

Fig. 4. Transmission and reflection spectra of a typical Sb_2S_3 thick film (576 nm).

Fig. 3a and Fig. 3b show the reflection R and the transmission T spectra as a function of wavelength for undoped and Sn-doped Sb_2S_3 samples. The presence of the maxima and minima of the reflectance spectrum at the same wavelength positions indicates the optical homogeneity of the deposited films and that no scattering or absorption occurs at long wavelengths. Two regions are indicated in Fig. 4; (I) A strong absorption region is observed in the optical range 400–650 nm. The values of the absorption coefficient, α, in this region were derived from the transmittance and reflectance spectra; (II) A weak absorption region in the optical range 650–1800 nm was also apparent, in which the absorption coefficient, α, was treated according in [5].

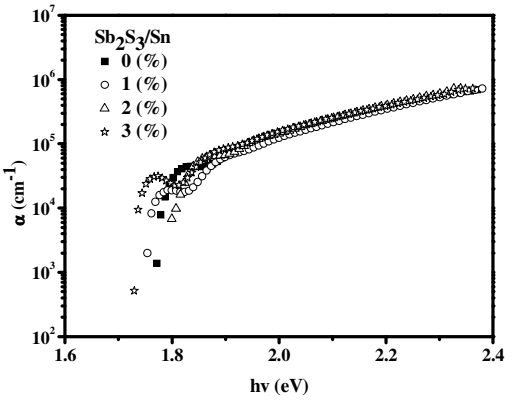

Fig. 5. Absorption coefficient α of undoped and Sn-doped Sb_2S_3 thin films

To calculate the absorption coefficient α (hν), the following relation was used [11, 12], which reads

$$\alpha = \frac{1}{d} Ln[\frac{(1-R)^2}{T}]$$

where d is the film thickness. The variation of the absorption coefficient, α, as a function of the photon energy for Sb_2S_3 films for Sn % molecular weight are presented in Fig. 5. It can be seen that all the films have relatively high absorption coefficients (10^4- 10^5 cm^{-1}) in the visible range and near-IR spectral range. This result is very important since the spectral dependence of the absorption coefficient affects the solar conversion efficiency in the case if this material was used as absorber in the solar cells [13]. Plotting of $(\alpha h\upsilon)^2$ versus photon energy, hυ, yields two direct allowed transition are observed : Eg_1 and Eg_2 (Fig. 6), the first indicating the direct optical transition, the second confirms the amorphous phase of the substratum. The two direct band gap Eg_1 and Eg_2 energy, estimated by a least-squares fit, increases from 1.78 to 1.98 eV and decreases from 1.92 to 1.96 eV respectively with increasing the Sn % molecular weight (see Fig. 7). It is known from the dispersion theory that in the region of low and medium absorption the index of refraction n is given in a single oscillator model by the expression [14]

$$n = \left[N + \left(N^2 - S^2 \right)^{\frac{1}{2}} \right]^{\frac{1}{2}} , \quad (1)$$

Where

$$N = 2S\frac{T_M - T_m}{T_M T_m} + \frac{S^2 + 1}{2} \quad , \tag{2}$$

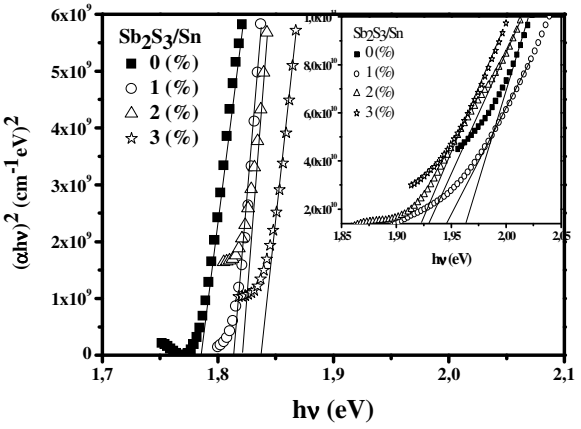

Fig. 6. A plot of $(\alpha h\nu)^2$ versus the photon energy ($h\nu$) of undoped and Sn-doped Sb_2S_3 thin films.

S is the refractive index of the glass substrate and T_M and T_m represent the envelopes of the maximum and minimum positions of the transmission spectra.

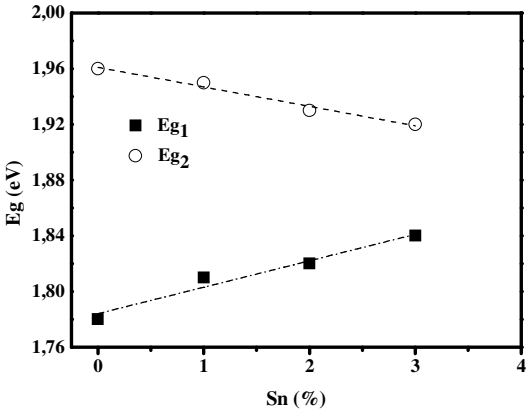

Fig. 7. Band gap energies Eg_1 and Eg_2 dependence of undoped and Sn-doped Sb_2S_3 thin films.

Fig. 8 shows the spectral response of the real parts of extinction coefficient, k and the refractive index, n the for the undoped and Sn-doped Sb_2S_3 thin films as a function of wavelength. The refractive index is found to decrease with an increase of the wavelength of the incident photon. At higher wavelengths of the incident photon, the refractive index, n, tends to a constant. The extinction coefficient, $k = \alpha\lambda/4\pi$. The refractive index decreases from a value of 3.2 - 2.8 at $\lambda = 0.7$ μm reaching a values of (2.9 - 2.7) at $\lambda = 1$

μm. At higher wavelengths, the refractive index n reached constant values of about 2.9 - 2.7 and k is negligible. It is clear that the refractive index increases by increasing the Sn content. So the films become more opaque.

3.3. Refractive index dispersion analysis

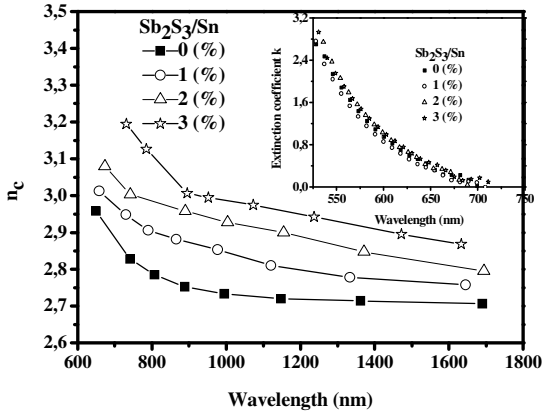

Fig. 8. Extinction coefficient k and Refractive index n of undoped and Sn-doped Sb_2S_3 thin films.

Wemple and DiDomenico [15] have developed a model where the refractive index dispersion is studied in the region of transparency below the gap, using the single-effective oscillator approximation. Defining two parameters, the oscillator energy, E_o and the dispersion energy E_d this model concludes that:

$$n^2(h\nu) = 1 + \frac{E_d E_0}{E_0^2 - (h\nu)^2} \quad , \tag{3}$$

Both Wemple parameters can be obtained from the slope and intercept of the plot $(n^2\text{-}1)\text{-}1 = f((h\nu)^2)$ with the y-axis as shown in Fig. 9. For further analysis of the optical data, the contribution from the free carrier electric susceptibility χe to the real dielectric constant is discussed according to the Spitzer–Fan model by [16]

$$\varepsilon_r = n^2 - k^2 = \varepsilon_\infty - \left(\frac{e^2}{\pi c^2}\right)\left(\frac{N}{m^*}\right)\lambda^2 \tag{4}$$

$$\left(\frac{e^2}{\pi c^2}\right)\left(\frac{N}{m^*}\right)\lambda^2 = -4\pi\chi_e \tag{5}$$

where ε_∞ is the high-frequency dielectric constant in the absence of any contribution from free carrier, χ_e is the electric free carrier susceptibility, N/m* is the carrier concentration to the effective mass ratio, e is the electronic charge, and c is the velocity of light. Plotting εr versus λ^2 (Fig. 10) and fitting to a straight line, the values of N/m* and ε_∞ were estimated. It is significant to compare the values of ε_∞ achieved from the Wemple–DiDomenico model (Fig. 8) with that obtained from the Spitzer-Fan model (Fig. 10), as they show satisfactory agreement. Fig. 11 shows $(-4\pi\chi e)$ versus λ^2. The figure depicts that χ_e increases in magnitude with the wavelength and becomes sufficiently large to reduce the refractive index and dielectric constant in the near-infrared region. A good fit to a straight line is seen from which the free carrier susceptibility values at the extremes of the investigated range were estimated.

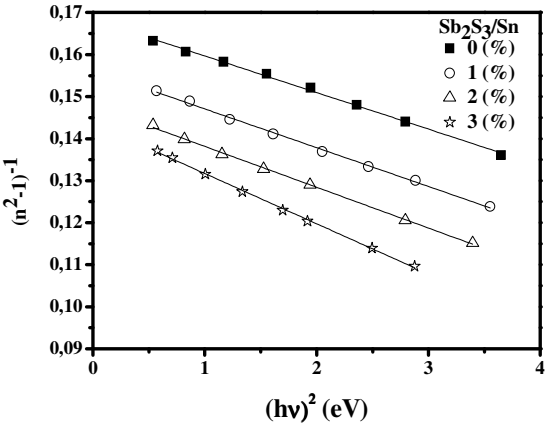

Fig. 10. A plot of $(n^2-1)^{-1}$ versus photon energy squared $(h\nu)^2$ of undoped and Sn-doped Sb_2S_3 thin films.

The values of Wemple-DiDomenico dispersion parameters, E_o, E_d static refractive index, n_o (calculated extrapolating the Wemple-DiDomenico) optical-dispersion equation to, $h\nu\rightarrow\infty$; ($n_o= 1+E_d/E_o$) as well as static dielectric constant, ε_r for the undoped and Sn-doped Sb_2S_3 thin films are listed in Table 2. The oscillator energy E_o is related by an empirical formula to the optical gap value: $E_o \approx 2Eg$ [15]. The calculated values of the optical band gap are also presented in Table 2.

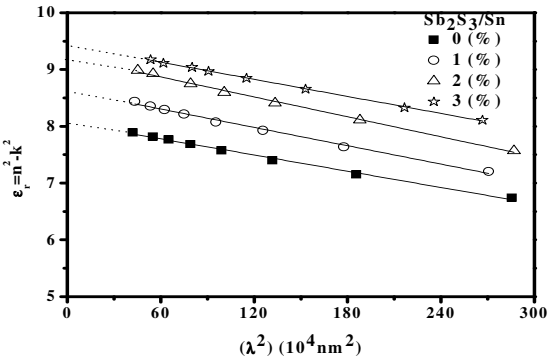

Fig. 11. A plot of the optical dielectric constant $\varepsilon r=n^2-k^2$ versus wavelength squared λ^2 of undoped and Sn-doped Sb_2S_3 thin films.

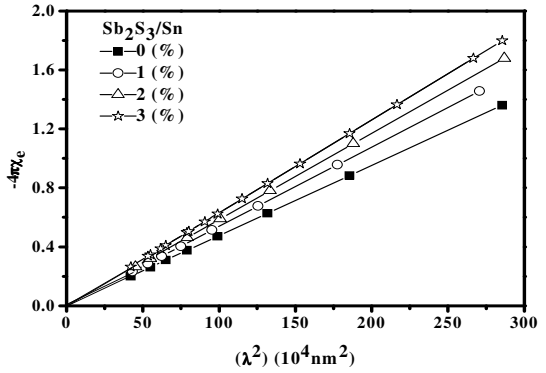

Fig. 12. A plot of (−4πχe) versus wavelength squared λ2 of undoped and Sn-doped Sb_2S_3 thin films.

Sb_2S_3/Sn	*E_0 (eV)*	*E_d (eV)*	*n(0)*	*$\varepsilon_{\infty sf}$*	*$\varepsilon_{\infty wd}$*	*E_g^{dir}* (eV)	*E_0 / E_g^{dir}*	*(N /m*) (*10^{48}cm^{-3})*	*-χ_e (*10^{-2})*
0 (%)	**4.39**	**26.15**	**2.70**	**8.06**	**7,82**	**1,96**	**2,23**	**1.75**	**1.57~10.74**
1 (%)	**4.11**	**26.39**	**2.75**	**8.62**	**8.13**	**1,95**	**2,10**	**1.97**	**1.83~11.54**
2 (%)	**3.89**	**26.48**	**2.79**	**9.22**	**9.01**	**1,93**	**2,01**	**2.15**	**2.07~13.29**
3 (%)	**3.46**	**24.24**	**2.87**	**9.42**	**9.13**	**1,92**	**1,80**	**2.31**	**2.62~13.29**

Table 2. The estimated values of the oscillator parameters E_0 and E_d, the value of the refractive index, n(0), and ε∞ as well as other related optical parameters extrapolated from the Wemple–Di Domenico model

4. Conclusion

Good-quality Sn-doped Sb_2S_3 thin films have been successfully deposited on heated glass substrates using the double-source thermal evaporation method. The refractive index, n, and extinction coefficient, k, of the Sb_2S_3/Sn films determined from the transmission and reflection spectra, recorded data over the wavelength range 300–1800 nm, were found to be dependant of the Sn % molecular weight. The values of n decrease from 3.2–2.8 at λ=0.7 μm to 2.9–2.7 at λ=1 μm and reach a constant value of 2.9 – 2.7 at higher wavelengths. All the films have relatively high absorption coefficients (10^4- 10^5 cm^{-1}) in the visible range and near-IR spectral range. The refractive index dispersion parameters were successfully calculated using the values of the high-frequency dielectric constant; the carrier concentration to the effective mass ratio and the electric free carrier susceptibility were also determined using the Spitzer-Fan model. Determination of these parameters may help in technological applications of Sb_2S_3 in thin film form. It is clear that by increasing the Sn content the carrier concentration to the effective mass ratio increases and we hope that by increasing more the Sn content to obtain Sn-doped Sb_2S_3 thin films with higher conductivity.

References

[1]K.Petkov, R. Todorov, D. Kozhuharova, L. Tichy, E. Cernoskova, P. J. S. Ewen. Changes in the physicochemical and optical properties of chalcogenide thin films from the system As-S and As-S-Tl. *J. Mat. Sci*. 2004;**39**:96–8.

[2]E.Marquez, A. M. Bernal-Oliva, J. M. Gonzales-Leal, R. Pietro-Alcon, T. Wagner. Optical properties and structure of amorphous (As0.33S0.67)100-xTex and GexSb40-xSx0 chalcogenide semiconducting alloy films deposited by vacuum thermal evaporation.J. *Phys. D: Appl. Phys*. 2006; **39**:1793–7.

[3]Q.Lu, H.Zeng, Z.Wang, X.Cao, L. Zhang.Design of Sb_2S_3 *nanorod-bundles: imperfect oriented attachment. Nanotechnology* 2006;**17**:2098–7.

[4]Z.S.El Mandouh, S.N.Salama.Some physical properties of evaporated thin films of antimony trisulfide.*J.Mat.Sci*. 1990;**25**:1715–4.

[5]F. Aousgi, M.Kanzari.Study of the optical properties of the amorphous Sb2S3 thin films Journal of Optoelectronics and Advanced Materials 2010;**12**:227–6.

[6]M.T.S. Nair, Y.Pena, J. Campos, V.M Garica, P.K. Nair. ChemInform Abstract: Chemically Deposited Sb2S3 and Sb2S3—CuS Thin FilmsJ. Electrochem. Soc.1998; **145**: 2113–8.

[7]A. Gassoumi, M. Kanzari and B. Rezig.Thermally induced changes in optical and electrical properties of thin $SnSb_2S_4$ films. Eur. Phys. J. Appl. Phys. 2008;41:**91**–5.

[8]O. S. Heavens, *Optical Properties of Thin Solid Films*, Butterworths, London; 1955.

[9]N.Tigau, V.Ciupina, G. Prodan. Structural, optical and electrical properties of Sb_2O_3 thin films with different thickness. J. Optoelect. Adv. Mater. 2006;**8**:37–6.

[10]Nicolae Tigau. Influence of temperature on the microcrystalline structure of thermally evaporated Sb_2S_3 thin films. Rom. Journ. *Phys.* 2008;**53**:209–7.

[11] M.Kanzari and B.Rezig. Effect of deposition temperature on the optical and structural properties of as-deposited CuInS2 films. *Semicond. Sci. Technol.* 2000;**15**:335–6.

[12]T.M.Wang, S.K. Zheng, W.C. Hao, C. Wang. Studies on photocatolytic activity and transmittance spectra of TiO2 thin films prepared by rf magnetron sputtering method. *Surf. Coat. Technol*.2002;**155**:141–5.

[13] A.M.Farid. Effect of Ag Content on the Optical Properties of a- Ge15 Se85-x Agx Alloys. *Egypt. J. Sol.*2002;25:23–10.

[14] J. I.Pankove, *Optical processes in semiconductors*, Prentice-Hall, New Jersey; 1971.

[15]S.H.Wemple, M.DiDomenico. Behavior of Electronic Dielectric Constant in Covalent and Ionic Materials. *M*. Phys. Rev., B3 1971;4:1338–14.

[16]W.G.Spitzer, H.Y. Fan. Determination of Opticals and Carrier Effective Mass of Semiconductors. *Phys. Rev*. 1957;**106**:882–9.